Metastable phases formed by ion mixing in the Hf-Nb system with a positive heat of formation

Metastable phases formed by ion mixing in the Hf–Nb system with a positive heat of formation

O Jin†, Y Ye and B X Liu†

Department of Materials Science and Engineering, Tsinghua University, Beijing 100084, People's Republic of China

Abstract. Amorphization was achieved in the Hf–Nb system with a positive heat of formation ($+6$ kJ mol^{-1}) by room-temperature 200 keV xenon ion mixing of multilayered films. On the basis of thermodynamic calculation, in which the interfacial free energy of multilayered films was specially taken into account, a Gibbs free-energy diagram was constructed and a relevant interpretation to the observed amorphization behaviour was proposed together with the kinetic considerations for the ion irradiation process. Also, two metastable FCC phases of Nb-rich and Hf-rich concentrations with different sizes were obtained by ion mixing.

1. Introduction

Since the 1960s [1], amorphous alloys have long been attractive, because they are expected to feature many novel properties. To produce more new amorphous alloys, various techniques have been developed, such as rapid quenching of the melts and pulsed-laser surface treatment, and have stimulated the progress of the alloy phase theory under non-equilibrium conditions. Ion beam mixing of alternately deposited metal–metal multilayered films has flourished since the 1980s and many metastable alloys of either amorphous or crystalline structure have been obtained by ion mixing [2, 3]. As its effective cooling rate can reach as high as 10^{14} K s^{-1} and its experimental parameters are easy to control, ion mixing is possible not only to synthesize new metastable alloys but also to trace the phase evolution experimentally by increasing the irradiation dose stepwise and thus to give insight into the underlying mechanism.

To date, metastable phase formation has been studied by ion mixing in more than 70 binary metal systems, among which most of the systems had a negative heat ΔH_f of formation. As it was generally thought that metastable phases, especially amorphous alloys, were easier to obtain in the negative-ΔH_f systems, the systems with positive ΔH_f have been less investigated [4, 5] and so far the experimental results have not all been in accordance with the predictions by some of the proposed models [6, 7]. There is no doubt that the alloying behaviour induced by ion mixing in such positive-ΔH_f systems is worth further study, not only experimentally but also theoretically, to gain a better understanding of the metastable phase formation mechanism for the binary metal systems, and it will hopefully have some impact on the progress of the non-equilibrium alloy phase theory.

† Also at China Centre of Advanced Science and Technology (World Laboratory) PO Box 8730, Beijing 100080, People's Republic of China.

In one of our previous studies of the Zr–Nb system with $\Delta H_f = +6$ kJ mol^{-1} [5], it was found that amorphization could be achieved by ion mixing; yet the composition range favouring amorphization was discontinuous, i.e. close to the Zr and Nb ends. Being in the same group as zirconium in the periodic table, hafnium is also of HCP structure at room temperature and the Hf–Nb system equally has $\Delta H_f = +6$ kJ mol^{-1}. It is naturally of interest to investigate whether a similar alloying behaviour will be exhibited in the Hf–Nb system.

In the present paper, we report the phase changes in the Hf–Nb multilayered films induced by 200 keV xenon ion mixing at room temperature. The observed amorphization behaviour is discussed on the basis of a thermodynamic calculation, with emphasis on the interfacial free energy involved in the multilayered films, which has sometimes been omitted.

2. Experimental procedure

Hf–Nb multilayered films were prepared by depositing alternately pure hafnium (99.9%) and pure niobium (99.9%) onto NaCl single-crystal substrates in an electron-gun evaporation system with a vacuum level of the order of 10^{-5} Pa. The total thickness of the films was about 50 nm, which approximately corresponded to the projected range plus projected range straggling of the irradiation ions, i.e. 200 keV xenon ions. The number of layers for each sample was seven or eight and the thickness of each layer varied according to the desired composition. As-deposited films were then irradiated in an implanter at room temperature by 200 keV xenon ions to doses from 5×10^{14} to 7×10^{15} Xe$^+$ cm^{-2}. The vacuum level during irradiation was better than 5×10^{-4} Pa and the ion current density was less than 1 μA cm^{-2} to minimize the heating effect. All samples were investigated by transmission electron microscopy (TEM) observations and selected-area diffraction (SAD) to identify the structure of the resultant phases. Energy-dispersive spectrum analysis, with an experimental error of 5%, was employed to determine the average compositions of the as-deposited films, as well as the real compositions of the ion-mixed phases in the irradiated samples.

Table 1. Number of layers and phase changes in the Hf–Nb multilayered films upon room-temperature 200 keV xenon ion mixing: FCC-I refers to a Nb-rich MX phase of FCC structure with a lattice parameter around 4.25 Å, while FCC-II refers to a Hf-rich MX phase also of FCC structure with a lattice parameter of around 4.55 Å; ——, no data obtained.

| Samples | Number of layers | Phase changes for the following doses | | | |
		5×10^{14} Xe$^+$ cm^{-2}	1×10^{15} Xe$^+$ cm^{-2}	3×10^{15} Xe$^+$ cm^{-2}	7×10^{15} Xe$^+$ cm^{-2}
Hf$_{17}$Nb$_{83}$	8	FCC-I	FCC-I	FCC-I	FCC-I
Hf$_{27}$Nb$_{73}$	8	FCC-I+FCC-II	FCC-I+FCC-II	FCC-I+FCC-II	FCC-I+FCC-II
Hf$_{40}$Nb$_{60}$	7	Amorphous+FCC-I	Amorphous+Nb	FCC-I	FCC-I
Hf$_{48}$Nb$_{52}$	7	FCC-I	FCC-I	FCC-I	FCC-I+*Amorphous*
Hf$_{60}$Nb$_{40}$	7	FCC-II+Nb	Amorphous+Nb	Amorphous+FCC-I	Amorphous+FCC-I
Hf$_{75}$Nb$_{25}$	8	FCC-II	Amorphous	Amorphous+FCC-II	Amorphous
Hf$_{90}$Nb$_{10}$	8	FCC-II+Nb	FCC-II+Nb	—	—

3. Results and discussion

3.1. Amorphization induced by ion mixing

Table 1 lists the phase changes in the Hf–Nb multilayered films under room-temperature 200 keV xenon ion irradiation. One sees that, in the four samples with a Hf concentration ranging from 40 to 75 at.%, amorphization was achieved, and that a unique amorphous phase was obtained in the Hf-rich sample, i.e. $Hf_{75}Nb_{25}$, at two irradiation doses of 1×10^{15} and 7×10^{15} Xe^+ cm^{-2}, as evidenced by the typical SAD pattern shown in figure 1. These results suggested that the amorphous phase was more inclined to form when the alloy composition was chosen to be Hf enriched.
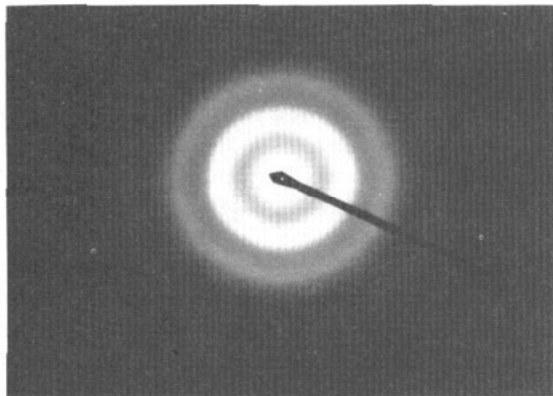

Figure 1. SAD pattern of the amorphous phase obtained in the $Hf_{75}Nb_{25}$ sample by room-temperature 200 keV xenon ion mixing at the dose of 1×10^{15} Xe^+ cm^{-2}.

In an attempt to reveal the thermodynamic driving force responsible for the observed amorphization behaviour in this system, the free-energy curve of the amorphous phase was calculated and compared with the initial energy state of the multilayered films for which the excess interfacial free energy was calculated [8] and included. The calculation of the free energy of the amorphous phase was on the basis of a model given by Miedema *et al* [8] and a method proposed by Alonso *et al* [9], described as follows:

$$\Delta G_{\text{amorphous}} = \Delta H^c + \alpha(X_A T_{m,A} + X_B T_{m,B}) - T\Delta S \tag{1}$$

where ΔH^c is a chemical contribution to the enthalpy of formation which takes into account the electron redistribution generated at the surface of contact between dissimilar atomic cells, α is an empirical constant equal to 3.5 J mol^{-1} K^{-1}, X_i and T_{mi} are the atomic concentration and melting point, respectively, of the constituent metals (of Hf and Nb in this case). T is the room temperature, equal to 300 K, and ΔS is the entropy of formation, taken to be that of an ideal solid solution as a first approximation.

The energy state of the as-deposited A–B multilayered films was calculated by adding the interfacial free energy to the ground state taken to be that of the bulk crystalline A+B mixture. For a binary metal system which has a positive ΔH_f, as the free energy of the alloy states is usually higher than that of a mixture of crystalline metals A and B in bulk form, any possible alloy is hardly obtainable through conventional techniques, e.g. liquid melt quenching. However, in the case of ion mixing of multilayered films, they certainly contain interfaces which are commonly regarded as transient layers of mixed A and B atoms

and possess excess free energy. As pointed out by Turnbull [10], the interfacial free energy can be divided into two parts, i.e. the physical and chemical contributions, written as

$$\gamma_{SS}^{AB} = \gamma_{SS}^{geo} + \gamma_{SS}^{chem}.$$ (2)

The physical contribution γ_{SS}^{geo} results from the elastic distortion of the atomic cells due to the difference of the atomic size and crystalline structure and its sign is always positive [11], while the chemical term γ_{SS}^{geo} originating from the redistribution of the electrons of the two metals has the same sign as the ΔH_f of the A–B system [12]. Thus the interfacial free energy should always be positive for those systems with positive ΔH_f, e.g. for the Hf–Nb system, and would definitely elevate the films to a higher energy level. By considering the interfacial energy, the Gibbs free energy of the multilayered films can then be calculated by [13]

$$\Delta G_{mul} = \alpha_A S_{fA} \gamma_{BA}^{SS} + \alpha_B S_{fB} \gamma_{AB}^{SS}$$ (3)

where S_{fA} and S_{fB} are the surface areas occupied by 1 mol of atoms A and B, being 2.54×10^5 m^2 and 2.20×10^5 m^2, respectively. The parameters α_A and α_B are the fractions of interfacial atoms A and B versus the total atoms in the multilayered films, respectively, which are geometrical parameters related to the film configuration and can be adjusted by changing the number of interfaces while the total thickness of the films is kept constant [14].

It should be mentioned that the above calculation was based on the semiempirical model and method, and the precision of the calculation certainly needs to be improved. However, our previous studies showed that such a calculation could give the semi-quantitative free-energy configuration of the phases concerned and the relative energy levels of the phases have been confirmed by steady-state thermal annealing of the corresponding multilayered films in some systems [15, 16]. In other words, such a calculation is able to give a relevant outline of the free-energy diagram. The details of the calculation procedure as well as the thermal annealing experiments for confirming the calculation can be found in our previous publications [13–16].

According to the calculation results, a free-energy diagram was constructed. For convenience, figures 2(*a*) and 2(*b*) exhibit the equilibrium phase diagram and the calculated free-energy diagram, respectively, of the Hf–Nb system. One sees from figure 2(*b*) that the free-energy curve of the amorphous phase is convex which is usually seen in positive-ΔH_f systems, and that the energy state of the multilayered films is displayed by an energy band instead of an energy curve, as the interface thickness was taken in range 4.5–5.5 Å in the calculation, considering the uncertainty in the experimental data [17]. The difference between the number of the layers (shown in table 1) and the actual configuration of the multilayered films was taken into account in the present calculation. The constructed diagram shows that, in the whole composition range, the Gibbs free energy of the multilayered films is comparable to that of the amorphous phase and the diagram can be divided into three portions along the concentration axis. In the two composition regimes towards the Nb and Hf ends (regimes I and II), the energy band of the multilayers is above the energy curve of the amorphous phase while, in the middle range of the diagram (regime III), the energy band intersects the energy curve of the amorphous phase due to the protrusion of the curve and the decrease in the band (multilayered films contained seven layers in this regime as listed in table 1). Firstly, we focus on the Hf-rich regime II. One can see from the figure that the calculated free energy of the multilayered films is about 5 kJ mol^{-1} higher than that of the amorphous phase, which can provide a driving force for amorphization. The Hf$_{75}$Nb$_{25}$ multilayered films did become amorphous upon ion mixing

to certain doses and a unique amorphous phase was obtained. For the $Hf_{90}Nb_{10}$ sample, because of the kinetic competition with a simple structured metastable FCC phase (to be discussed later), the amorphous phase failed to be formed. In other words, besides the thermodynamic driving force, the kinetic factor should also be taken into account when considering whether the amorphous phase can be formed or not. As has been discussed in [7], if there exists a crystalline phase of simple structure competing with the amorphous phase, amorphization will be hindered, as this crystalline phase is able to nucleate and grow within the relaxation period in the ion irradiation process. This is why no amorphous phase was obtained in the $Hf_{90}Nb_{10}$ multilayered films, now in the $Hf_{17}Nb_{83}$ and $Hf_{27}Nb_{25}$ samples in regime I, although the thermodynamic conditions were similar to those of $Hf_{75}Nb_{25}$ films. Instead of an amorphous phase, two metastable crystalline (MX) phases both of simple FCC structure were obtained in these three films by ion mixing as indicated in table 1.

Table 2. The indexing results of the MX phase of FCC structure obtained in the $Hf_{17}Nb_{83}$ sample by room-temperature 200 keV xenon ion mixing at a dose of 3×10^{15} Xe^+ cm^2. Lattice parameter $a = 4.19$ Å.

Planar spacing (experimental) (Å)	Planar indices hkl	Planar spacing (calculation) (Å)	Visual intensity of diffraction lines
2.42	111	2.42	Strong
2.09	200	2.10	Strong
1.48	220	1.48	Strong
1.27	311	1.26	Medium
1.21	222	1.21	Weak
1.05	400	1.05	Weak
0.96	331	0.96	Weak
0.94	420	0.94	Weak
0.86	422	0.86	Weak
0.81	333,511	0.81	Weak

Now we turn to the middle part of the diagram, i.e. regime III, in which the $Hf_{40}Nb_{60}$, $Hf_{48}Nb_{52}$ and $Hf_{60}Nb_{40}$ samples are included. Amorphization was observed in these samples, and an amorphous phase was formed coexistent with the crystalline phases. It could be interpreted that the interfacial free energy elevated the multilayered films to a high-energy state comparable to that of the amorphous phase, which provided the possibility of amorphization thermodynamically. However, as the driving force for amorphization was relatively small and competing MX phases exist, it might be difficult to form a unique amorphous phase in this composition regime.

3.2. MX phase formation

One also sees from table 1 that, in all the samples listed, MX phases of FCC structure were obtained at various irradiation doses. As neither Hf (HCP) nor Nb (BCC) is of FCC structure, they were no doubt metastable phases. According to the sizes, they were named FCC-I and FCC-II, with lattice parameters of around 4.25 Å and 4.55 Å, respectively, indicated in table 1. It is interesting to note that, in the two samples with the concentrations closest to the two constitutent metal ends among the studied films, i.e. in the $Hf_{17}Nb_{83}$ and $Hf_{90}Nb_{10}$ samples, a unique FCC phase with a lattice parameter of 4.19 Å and another FCC phase with a lattice parameter of 4.57 Å, respectively, coexistent with Nb, were obtained at
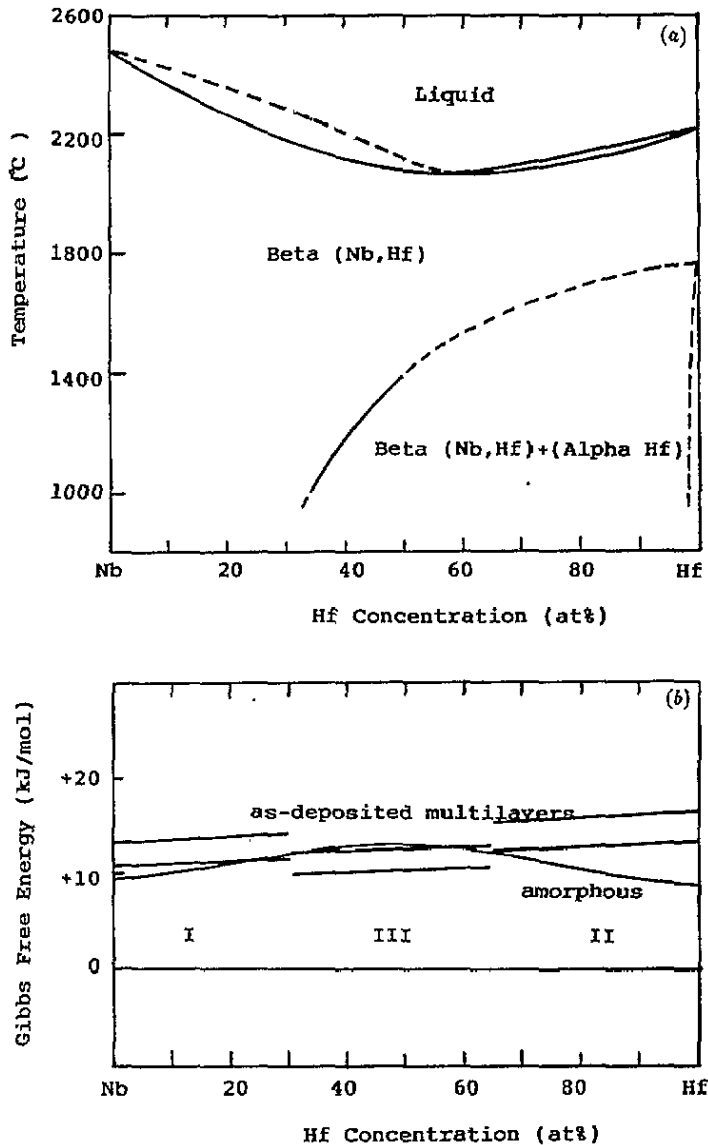
Figure 2. (*a*) Equilibrium phase diagram of the Hf–Nb system. (*b*) Constructed Gibbs free-energy diagram of the Hf–Nb system including an energy curve of amorphous phase and an energy band of the as-deposited multilayered films.

all irradiation doses. The SAD patterns of the two MX FCC phases are shown in figure 3 and their indexing results are listed in tables 2 and 3. It was obvious that the FCC-I phase was Nb rich, while the FCC-II phase was Hf rich. Under the assumption that the atomic volume was unchanged, the lattice parameters of the FCC phases formed by pure Nb and Hf were calcualted to be 4.17 Å and 4.47 Å, respectively, using the lattice parameters of the two metals of room-temperature crystalline structure. The calculated parameters agreed quite well with the experimental data. It is worth mentioning that, in our previous study in the Zr–Nb system [5], these two FCC MX phases were also obtained and their lattice parameters were almost the same as those obtained in the Hf–Nb system.
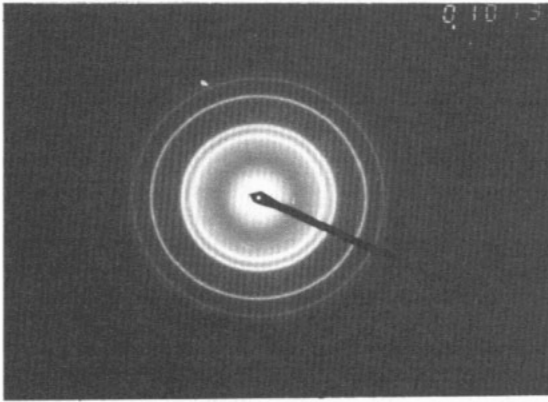
(a)
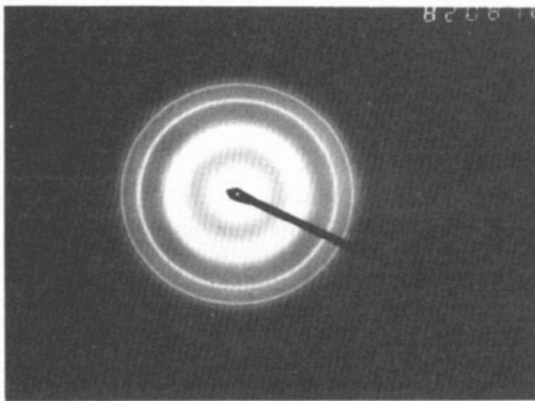
(b)

Figure 3. SAD patterns of the MX phases of FCC structure obtained in (a) $Hf_{17}Nb_{83}$ sample with a lattice parameter of 4.19 Å at an irradiation dose of 3×10^{15} Xe^+ cm^{-2}; (b) $Hf_{90}Nb_{10}$ sample with a lattice parameter of 4.57 Å at an irradiation dose of 1×10^{15} Xe^+ cm^{-2} by room-temperature 200 keV xenon ion mixing.

It is relevant that a FCC phase emerged at the hafnium end of the equilibrium phase diagram, as there only exists a stacking order difference between HCP and FCC structure and it is easy to transform from the HCP Hf to the FCC MX phase. However, as the FCC phase emerged at the niobium end, the transformation from BCC to FCC is not as simple as for the HCP–FCC transition. Recently, Zhang and Liu [18] reported the formation of a similar FCC MX phase in the Co–Nb system and an intermediate state of HCP phase for the transformation from BCC to FCC and thus proposed a reverse martensitic phase transformation mechanism of BCC→HCP→FCC on the basis of experimental observation

Table 3. The indexing results of the MX phase of FCC structure obtained in the $Hf_{90}Nb_{10}$ sample by room-temperature 200 keV xenon ion mixing at a dose of 1×10^{15} Xe^+ cm^{-2}. Lattice parameter $a = 4.57$ Å.

Planar spacing (experimental) (Å)	Planar indices *hkl*	Planar spacing (calculation) (Å)	Visual intensity of diffraction lines
2.65	111	2.64	Strong
2.45[a]	110[a]	2.45[a]	Medium[a]
2.27	200	2.29	Medium
1.63	220	1.62	Medium
1.38	311	1.38	Medium
1.32	222	1.32	Weak
1.14	400	1.14	Weak
1.05	331	1.05	Weak
1.02	420	1.02	Weak
0.94	422	0.93	Weak
0.88	333,511	0.88	Weak

[a] Nb data.

and crystallographic correlation. It is certainly of interest to study further whether such a two-step phase transition mechanism also applies to the Hf–Nb and the Zr–Nb systems.

4. Conclusion

(1) Amorphization was achieved in the Hf–Nb system by room-temperature 200 keV xenon ion mixing of multilayered films consisting of seven or eight layers in a Hf content range from 40 to 75 at.%; yet a unique amorphous phase was obtained in the multilayered films only near the composition $Hf_{75}Nb_{25}$. The major driving force for amorphization was the excess interfacial free energy in the films for this positive ΔH_f system.

(2) Two FCC MX phases were obtained in the Hf–Nb system by ion mixing with Nb-rich and Hf-rich compositions, respectively.

Acknowledgments

References

[1] Duwez P, Willens R H and Klement W 1960 *J. Appl. Phys.* **31** 1136
[2] Liu B X 1991 *Vacuum* **42** 75
[3] Blatter A and Allmen M V 1985 *Phys. Rev. Lett.* **54** 2103
[4] Huang L J and Liu B X 1987 *Nucl. Instrum. Methods* B **18** 256
[5] Jin O and Liu B X 1994 *J. Phys.: Condens. Matter* **6** L39
[6] Alonso J A and Simozar S 1983 *Solid State Commun.* **48** 765
[7] Liu B X 1986 *Phys. Status Solidi* a **94** 11
[8] Miedema A R, Niessen A K, deBoer F R, Boom R and Mattens W C M 1989 *Cohesion in Metals: Transition Metal Alloys* (Amsterdam: North-Holland)

[9] Alonso J A, Gallego L J and Simozar J A 1990 *Nuovo Cimento* **12** 587
[10] Turnbull D 1955 *Impurities and Imperfections* (Metals Park, OH: American Society of Metals) p 121
[11] Murr L E 1975 *Interfacial Phenomena in Metals and Alloys* (London: Addison-Wesley)
[12] Miedema A R 1978 *Z. Metallk.* **69** 455
[13] Jin O, Zhang Z J and Liu B X 1995 *J. Appl. Phys.* **78**
[14] Zhang Z J, Jin O and Liu B X 1995 *Phys. Rev.* B **51** 8076
[15] Liu B X and Zhang Z J 1994 *Phys. Rev.* B **49** 12519
[16] Zhang Z J, Bai H Y, Qiu O L, Yang T, Tao K and Liu B X 1993 *J. Appl. Phys.* **73** 1702
[17] Cui F Z, Fan Y D, Wang Y, Vredenberg A M, Draaisma H J G and Xu R 1990 *J. Appl. Phys.* **68** 701
[18] Zhang Z J and Liu B X 1994 *J. Phys.: Condens. Matter* **6** 2647